Study the amplication effect of different slope subject to seismic loading

Le Gao[1, *], Sizhe Huang[2]

[1]School of Civil Engineering and Water Resources, Qinghai University, Xining, China, 810016

[2]School of Civil Engineering and Transportation, South China University of Technology, Guangzhou, China, 510641

* Corresponding Author Email: 18254818611@163.com

Abstract. The dynamic response and instability mechanisms of slopes under the influence of strong earthquakes have always been crucial areas of research in geological hazards. This study aims to delve into the stability of various types of slopes under seismic conditions. Utilizing the finite difference method, it unveils the dynamic response patterns of different slope types.And using the controlled variable method, this study meticulously analyzed the acceleration, displacement, and dynamic stress response of slopes with different angles, clarifying the impact of slope angle and varying accelerations on slope dynamic responses. The findings are as follows: The Peak Ground Acceleration (PGA) of slopes increases with elevation, reaching its maximum at the slope crest. This coefficient decreases as the slope angle increases, exhibiting a pronounced tendency for acceleration to be more pronounced near the surface. Displacement peaks, particularly sensitive to changes in seismic acceleration within the relative elevation range of 0.6 to 0.8, decrease with an increase in slope angle, especially beyond 60°, at which point the displacement response mechanism undergoes a change. Stress peaks diminish with rising elevation and become more pronounced with increased seismic load, indicating that the upper parts of slopes are more significantly affected by earthquakes. The increase in slope angle shifts stress concentration from the mid-slope towards the toe, particularly under steep slopes, where stress at the slope foot notably increases.

Keywords: Slope, Dynamic response, Seismic wave, Stress analysis, Strain increment analysis, Numerical simulation

1. Introduction

Our country is located in the intersection of the Circum-Pacific Seismic Belt and the Eurasian Seismic Belt, where seismic activity is extremely intense [1, 2]. This has triggered numerous disasters, resulting in significant human and property losses. For example, the 2017 Jiuzhaigou earthquake led to extensive landslides, causing damage to 73,671 houses [3]. Currently, many major engineering projects, such as hydropower stations and bridge constructions, are built in the complex terrain of mountainous areas, inevitably facing the stability issues of slopes [4]. Due to the seismic nature of these mountainous regions, geological hazards are frequent, and earthquakes are one of the main factors inducing slope instability. Therefore, studying the dynamic response of different slopes under seismic actions and investigating the intrinsic factors influencing stability are of paramount importance. This research aims to guide engineering construction in light of seismic effects on slope stability.

Numerical simulation methods have gradually taken a dominant position in slope engineering due to their efficiency and cost-effectiveness. Bolla and Paronuzzi identified deficiencies in the pseudo-static method when analyzing the dynamic stability of rocky slopes [5]. Guo and Ge et al, utilized the VSAM method for seismic stability assessment [6]. Qi and He et al, proposed a graphical method for evaluating seismic slope stability using g-lines [7]. Fan and Li et al, emphasized the necessity of considering the influence of vertical seismic forces when analyzing seismic slope stability [8]. Wang et al, proposed the dynamic response mechanism and post-failure movement characteristics of earthquake-induced landslides in high-cold and high-altitude areas [9]. Khan and van der Meijde et al, investigated the amplification effects of terrain on seismic activity [10]. Liang and Cui et al, studied the significant control of fault activity and anticline evolution on the initiation location of seismic landslides [11]. Xu et al, pointed out that soft rock layers within the slope are a crucial factor leading to slope instability and failure [12]. Qi and He et al, explored how peak horizontal acceleration varies with elevation at a single slope angle. [13].

In this context, to further explore the impact of slope angle and earthquake intensity on slope failure, this article is based on numerical simulation methods, applied the controlled variable method to specifically investigate the dynamic responses of slopes with different angles under seismic activity, including changes in acceleration, displacement, and stress to provide reference for engineering applications.

2. Study area

The research area is situated in the middle reaches of the Jinsha River, as shown in figure 1,part of the Sichuan-Yunnan Block within the Qinghai-Tibet Plateau. Known for its intense tectonic activity, the region has experienced multiple earthquakes exceeding Ms7.0, making it one of the most seismically active zones in China. The area is characterized by numerous steep, high-layered slopes with slopes ranging from 40° to 60°. Rock types include thick-bedded sandstone, limestone, thin to extremely thin-bedded slate, and phyllite, categorized into hard to extremely hard rocks and soft rocks based on their strength. The slopes also feature rich joint and fracture systems. The physical and mechanical parameters of the slope are shown in Table 1.

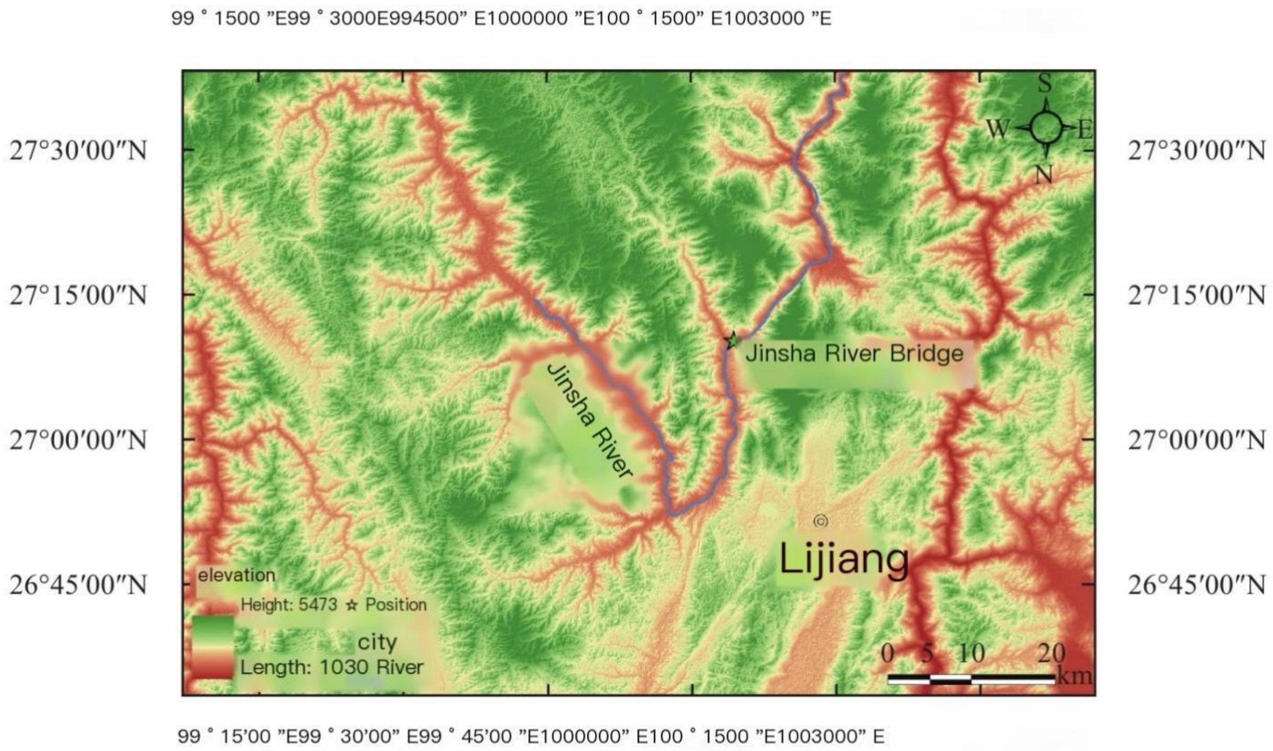

Figure 1. Geographical location of the study area

Table 1. Physical and Mechanical Parameters of Model Materials

Material	Bulk Density (kg/m^3)	Poisson's Ratio	Elasticity modulus (MPa)	Internal Friction Angle (°)	Cohesion (kPa)
Soft Rock	20.0	0.31	13.0	35.0	300.0

3. Numerical model setup

3.1. Software Brief Introduction

Flac3D is a computer software based on the Lagrangian algorithm, employing a continuous medium explicit finite difference approach. Positioned between finite element and discrete element methods, Flac3D is particularly suited for simulating large deformations and rotational distortions in geological materials.

3.2. Numerical Model Establishment and Parameter Configuration

This study utilizes a numerical model based on a typical homogeneous rock slope in the Jinsha River region of China, as the geological background. After appropriate generalization, the model shown in Figure 2 is established with dimensions of 120 m (length) × 50 m (height) × 20 m (width). To investigate the influence of slope topography on seismic amplification effects, the following computational conditions are set: maintaining a constant slope height of 50 m while varying slope angles at 30°, 45°, 60°, and 75°. The numerical model adopts free-field boundary conditions, as depicted in Figure 3, with seismic waves input from the bottom boundary. Fixed constraints are applied to the model's perimeter to eliminate distortion effects from boundary conditions on the propagation of plane seismic waves. Local damping is employed in dynamic calculations to dissipate kinetic energy generated during vibration, with a damping coefficient ultimately set to 0.1571.

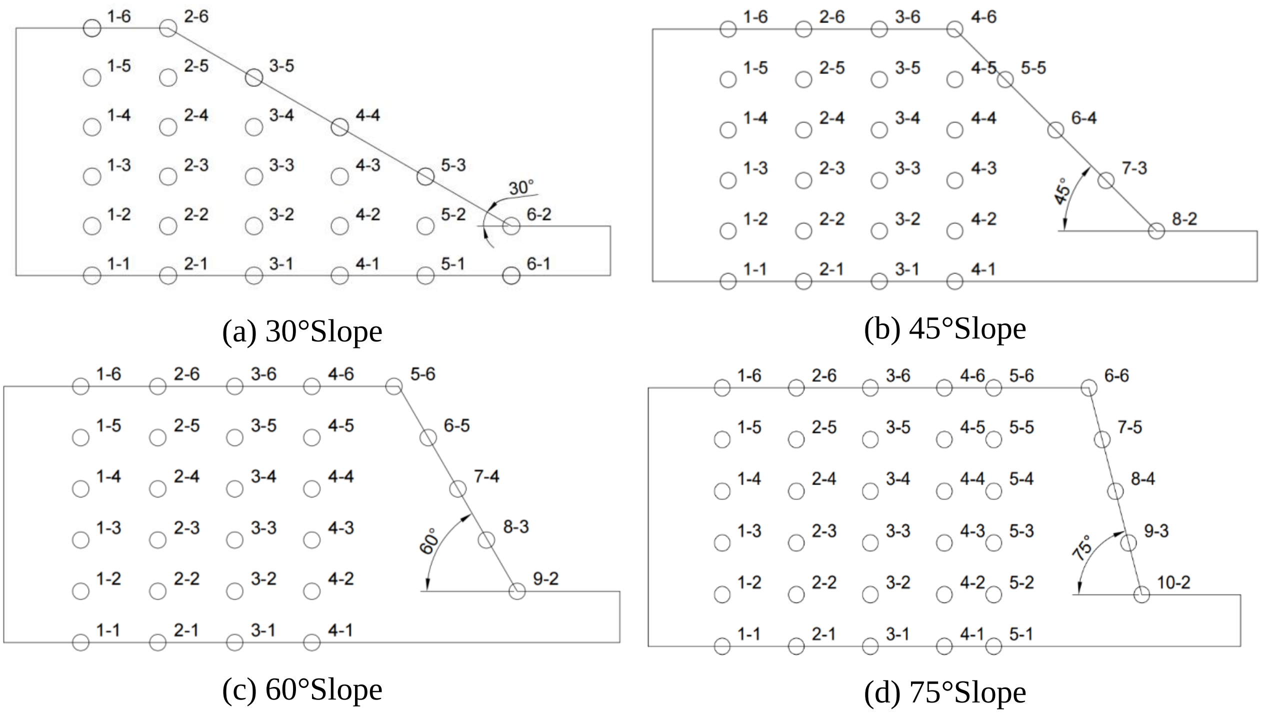

(a) 30°Slope (b) 45°Slope

(c) 60°Slope (d) 75°Slope

Figure 2. Calculation Model

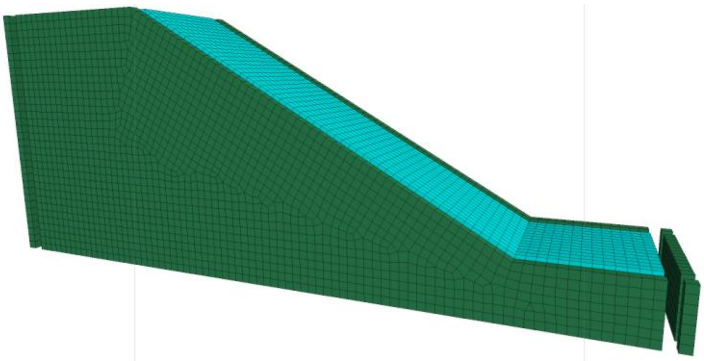

Figure 3. Free-field Boundary of Slope Model

3.3. Seismic Wave Loading

The seismic waves adopted in this study, along with their dynamic acceleration time history and the Fourier spectrum curve of acceleration, are depicted in Figure 4. The peak acceleration is 1 m/s², with a predominant frequency of 4.5 Hz. The input waves are subjected to baseline correction and filtering. Subsequently, their amplitudes are adjusted to 0.1g, 0.2g, 0.3g, and 0.4g according to loading requirements. The dynamic loads are applied vertically from the bottom boundary using the acceleration time history.

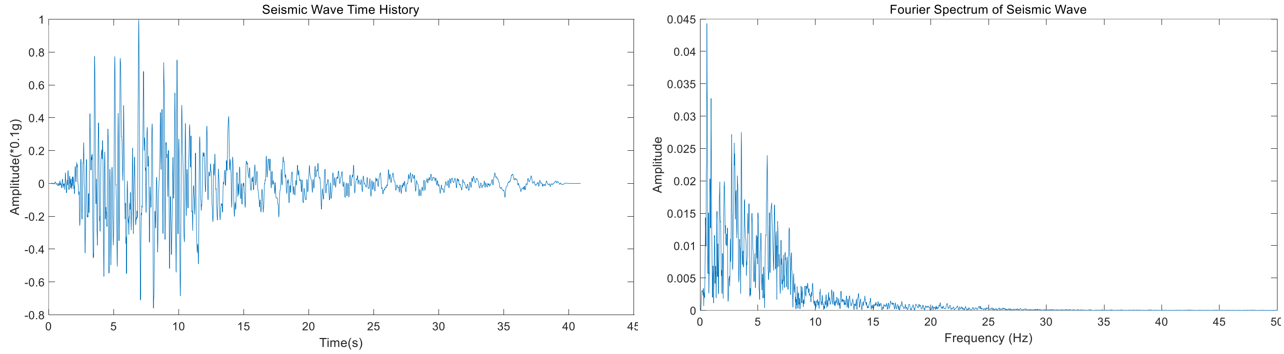

(a) Acceleration Time History (b) Acceleration Fourier Spectrum Plot

Figure 4. Acceleration Time History&Fourier Spectrum Plot

4. Result analysis

4.1. Acceleration responses

To better investigate the dynamic response patterns of slopes to seismic events, this paper introduces the concept of acceleration amplification factor for quantitative analysis. The acceleration amplification factor (PGA) is defined as equation (1):

$$PGA_i = \frac{a_i^{max}}{a_0} \tag{1}$$

In the equation, a_i^{max} represents the peak acceleration at detection point i , and a_0 represents the peak acceleration at the incident point.

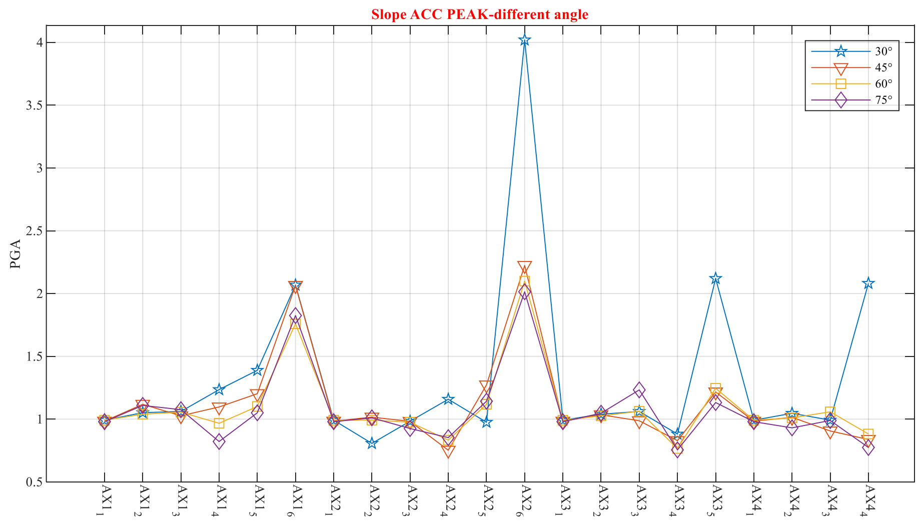

Figure 5. PGA of each monitoring point at different slope angles α

Figure 5. reveals that under various slope angles (∝)), the Peak Ground Acceleration (PGA) generally increases with elevation, with the maximum values consistently occurring at the slope crest, indicating a gradient increase in PGA from the base to the top of the slope. Additionally, the PGA

tends to decrease as the slope angle increases at any given location. At the same elevation, the PGA at slope surface monitoring points exceeds that of points located within the slope (with the maximum PGA values at different elevations respectively found at monitoring points AX2_6, AX3_5, AX4_4, AX5_3, AX6_2). As Figures 6(a), 6(b), and 6(c) demonstrate, at the same elevation, the closer to the slope surface, the greater the acceleration peak, reaching its maximum at the slope surface. This illustrates the pronounced tendency of acceleration to amplify closer to the surface.

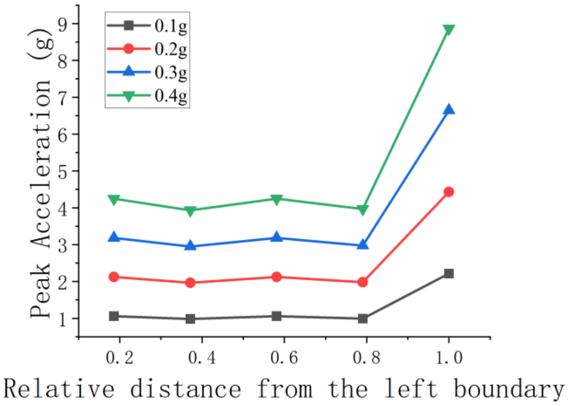

(a) At an elevation of 20 m

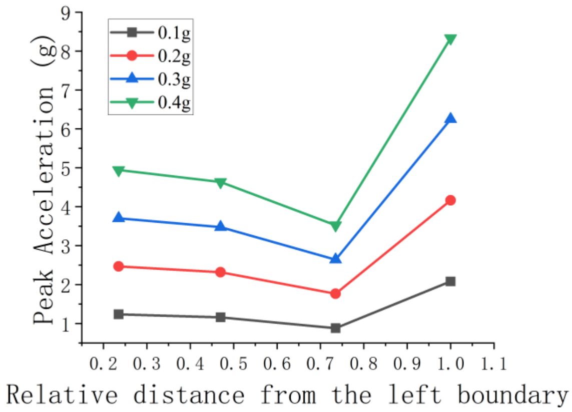

(b) At an elevation of 30 m

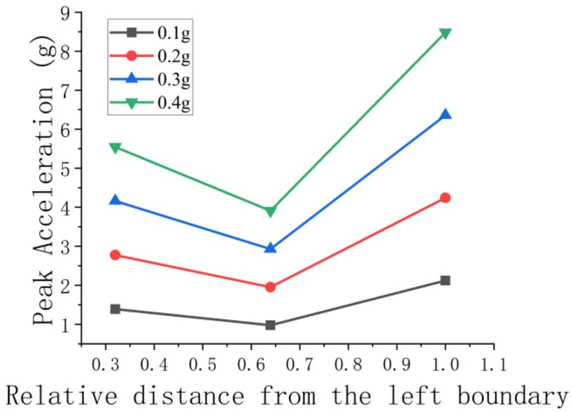

(c) At an elevation of 40 m

Figure 6. Peak change in acceleration in the horizontal direction

As depicted in Figures 7(a) and 7(b), in the upper and middle parts of the slope, the peak acceleration values show a decreasing trend with increasing slope angle, while changes in slope angle have little effect on the peak acceleration values in the lower parts of the slope. Figure 7(c) demonstrates that at the slope surface, the PGA first decreases and then increases with distance from the toe. At a slope angle of 30°, the minimum PGA occurs in the middle of the slope surface. As the slope angle increases, the position of minimum PGA gradually shifts from near the toe towards the shoulder, leading to a general decrease in the slope's overall acceleration. Changes in slope angle have a more significant effect on acceleration near the shoulder, with almost no impact near the toe.

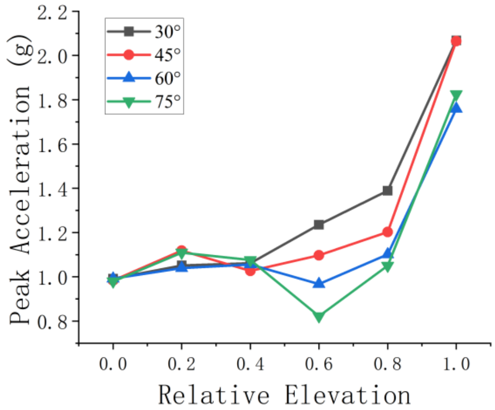

(a) Monitoring point 1_1:1_6

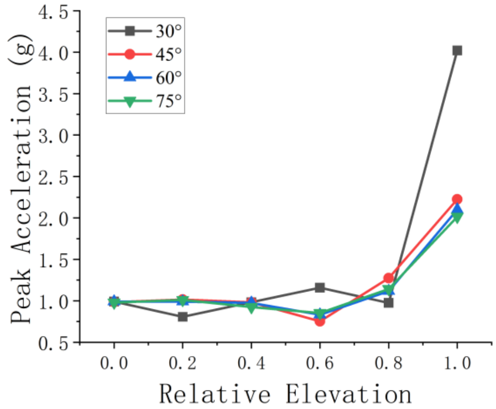

(b) Monitoring point 2_1:2_6

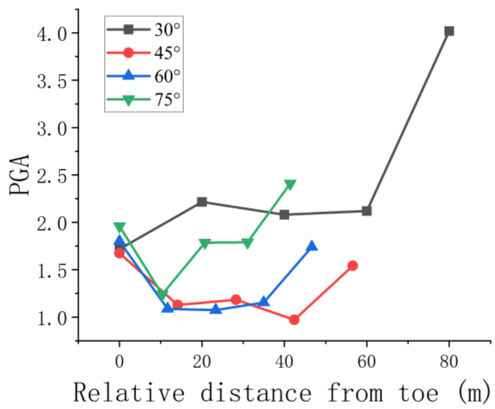

(c) Slope surface

Figure 7. Peak acceleration changes and PGA changes

As depicted in Figure 8, the maximum acceleration point of the slope is located at the crest. Taking a seismic load of 0.1g as an example, except for the slope angle of 75° where the peak acceleration occurs at monitoring point 6_6 (with a peak value of 2.41g), all other peak accelerations are found at monitoring point 2_6, with peak values of 4.02g at a slope angle of 30°, 2.22g at 45°, and 2.10g at 60°.

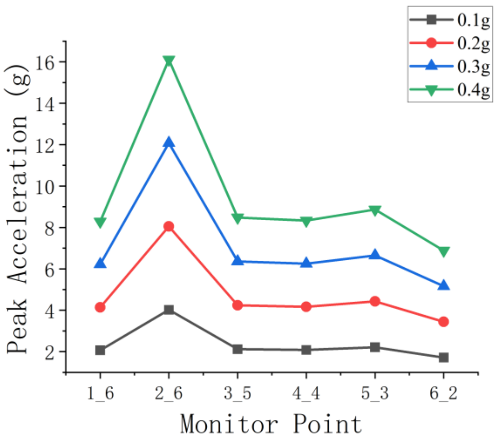

(a) 30° slope

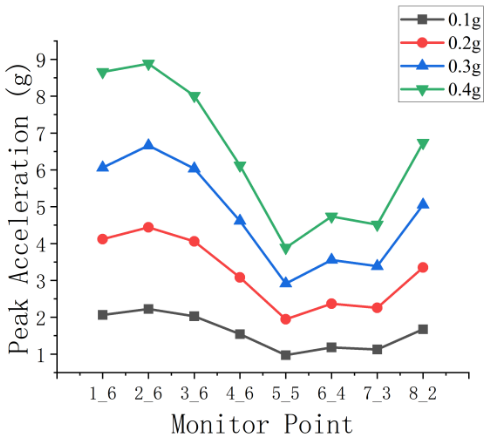

(b) 45° slope

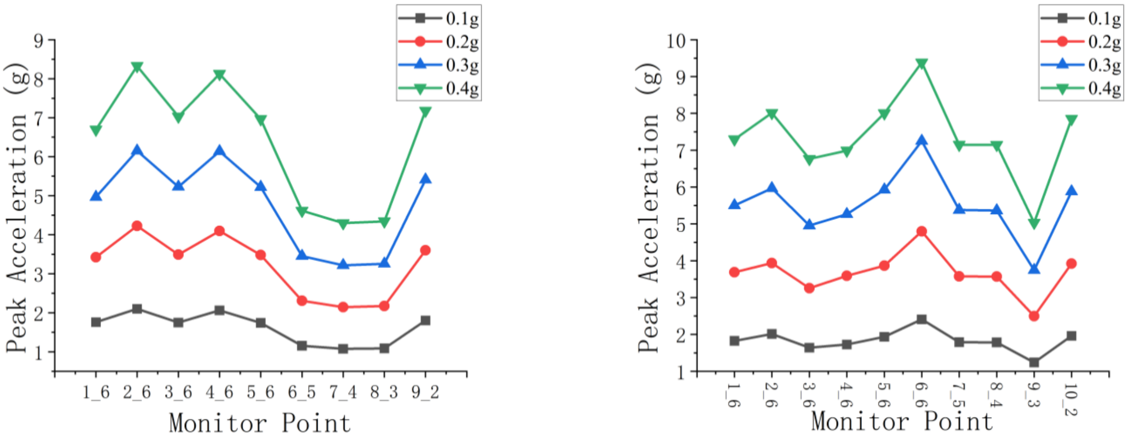

(c) 60° slope (d) 75° slope

Figure 8. Variations in Peak Acceleration of Slopes with Different Angles

4.2. Displacement responses

In all four different seismic acceleration scenarios (0.1g, 0.2g, 0.3g, 0.4g), a nonlinear elevation-displacement relationship is observed, where the peak displacement decreases at mid-relative elevations and then increases again with further elevation. For each given seismic acceleration, there is a distinct upward trend, especially between the later monitoring points, i.e., between relative elevations of 0.6 and 0.8, and this trend becomes more pronounced with increasing load intensity, as shown in Figure 9. This indicates that the displacement response in the upper-middle part of the slope is more sensitive to changes in seismic acceleration.

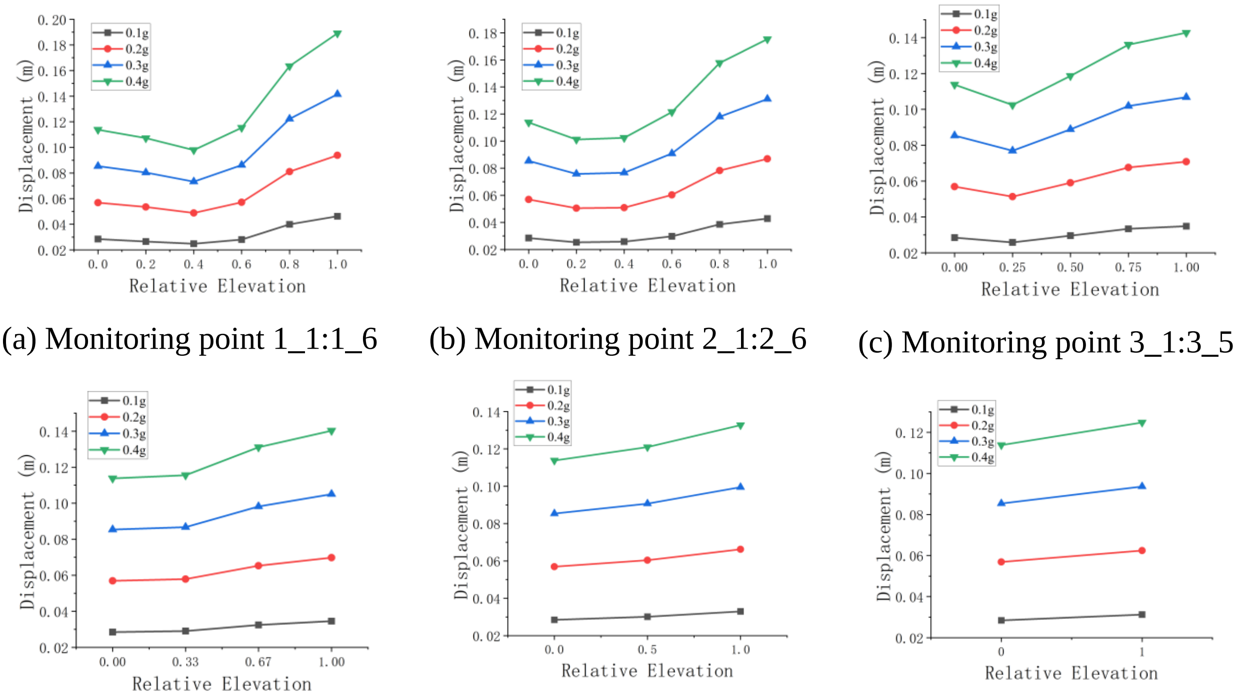

(a) Monitoring point 1_1:1_6 (b) Monitoring point 2_1:2_6 (c) Monitoring point 3_1:3_5

(d) Monitoring point 4_1:4_4 (e) Monitoring point 5_1:1_3 (f) Monitoring point 6_1:6_2

Figure 9. Elevation-Dependent Variation in Peak Displacement

Observing Figure 10 reveals that at the same elevation, as one moves closer to the slope surface, the peak displacement values increase, indicating a surficial trend. This trend is attributed to the lack of constraint near the slope surface, allowing materials to move more freely.

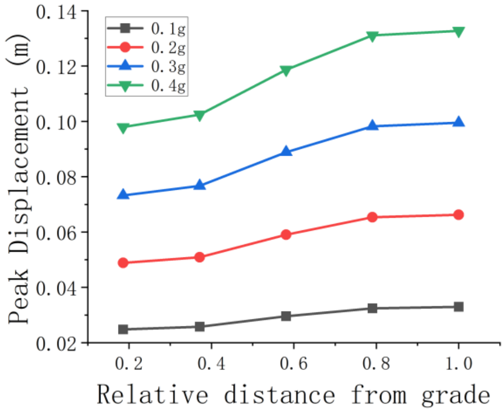

Figure 10. Horizontal Variation of Peak Displacement at a Constant Elevation Level

From Figure 11, it is evident that for slopes with angles less than 60°, the impact of different slope angles on displacement magnitude is most pronounced at the slope crest (relative elevation of 1), while it is minimal at the lower part of the slope body (relative elevation of 0.0 to 0.4). However, once the slope angle reaches 60°, further increases in slope angle do not significantly alter the displacement at the slope top (relative elevation of 1), especially in the middle part of the slope crest. Beyond a slope angle of 60°, the displacement mechanism near the middle part of the slope crest changes. As the slope angle increases, the peak displacement values tend to decrease with the increase in angle.

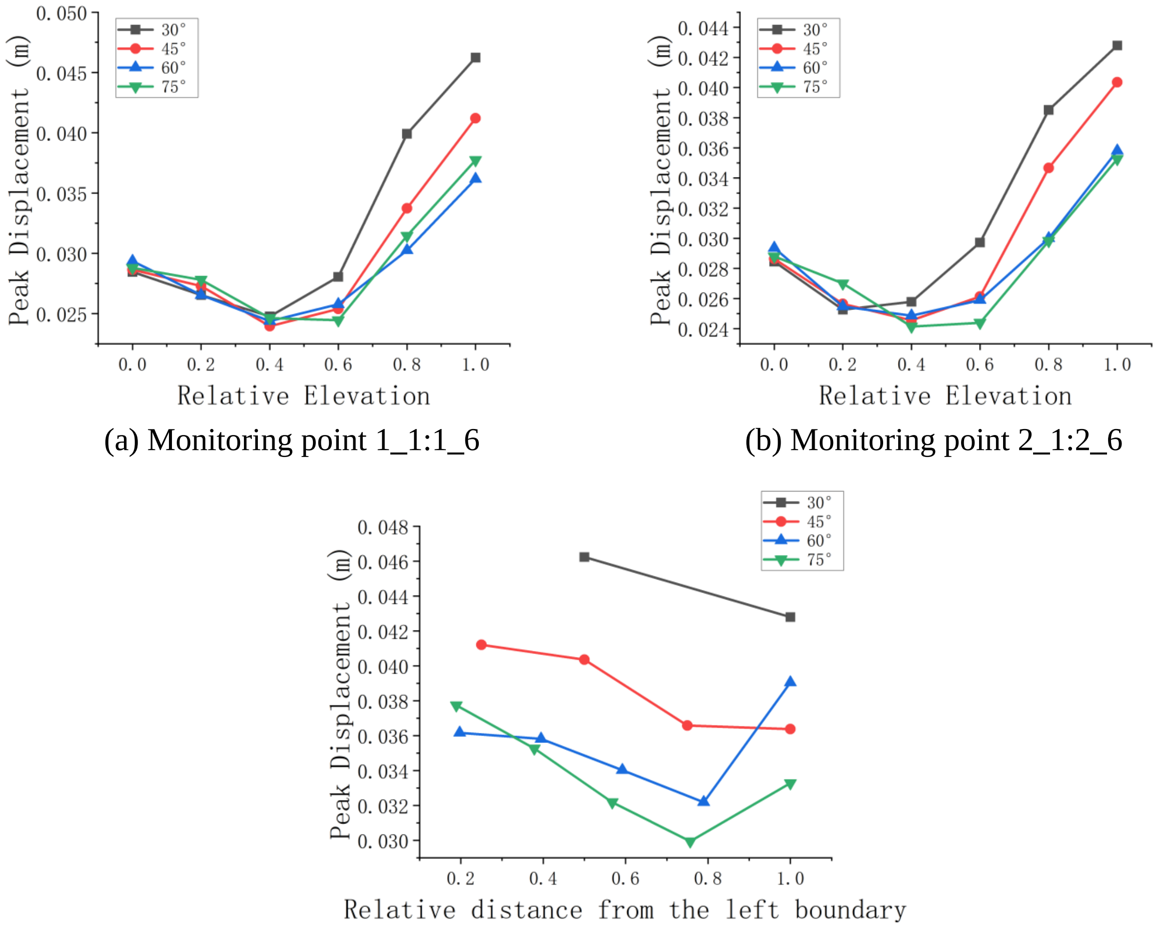

Figure 11. Distribution of Peak Displacement

Figure 12 shows that peak displacement decreases and then increases with distance from the slope's toe across all angles, suggesting a dynamic impact that weakens near the top and then intensifies due to seismic wave effects. Steeper slopes (75°) exhibit a significant rise in displacement further from the angle, while milder slopes (30° and 45°) show a more modest increase, indicating steeper slopes accumulate larger displacements at their ends, contrasting with the stability of gentler slopes under seismic activity. This pattern hints at slope angle influencing seismic wave amplification or attenuation, with steeper slopes causing more pronounced displacement at the crest through wave reflections and interference. Conversely, gentler slopes see a dispersed amplification effect, resulting in smaller peak displacements. Steep slopes may also focus seismic waves, leading to higher dynamic responses at specific points, whereas this effect is less marked on gentler slopes, causing minimal displacement increases far from the toe.

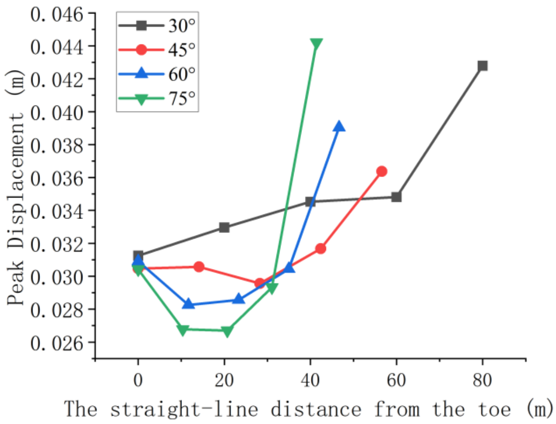

Figure 12. Variability in Peak Displacement Distribution Relative to the Distance from the Slope Toe

4.3. Stress analysis

In the study of the relationship between slope stress distribution and elevation, seismic loads ranging from 0.1g to 0.4g were applied, with results displayed in Figure 13. It was found that the peak stress values of the slope decrease gradually with elevation and that this variation becomes more pronounced with the increase in the intensity of the applied load. This is attributed to the top of the slope being closer to the free surface, where the material is less constrained near the free surface and thus can release energy through greater deformation, resulting in relatively lower peak stress values. Conversely, the bottom of the slope is subject to greater constraints, leading to stress concentration and, consequently, relatively higher peak stress values.

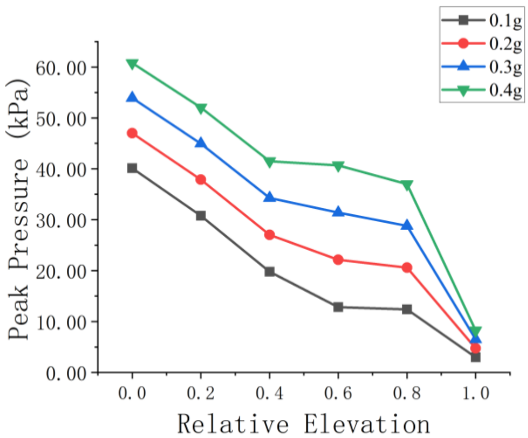

Figure 13. Variability in Peak Pressure Distribution Relative to the Elevation

According to Figure 14, the peak stress values for different slope angles are reached at different relative distances at the same elevation level. At the same elevation, as the slope angle increases, the area of stress concentration gradually shifts from the mid-slope towards the toe. The change in slope angle has a significant impact on the stress distribution near the base of the slope, while its effect on the internal parts of the slope is minimal.

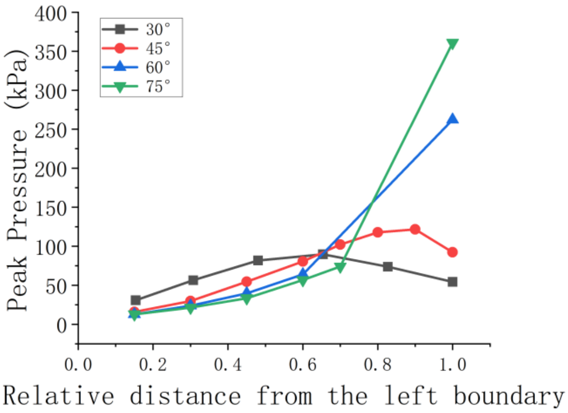

Figure 14. Horizontal Variation of Peak Pressure at a Constant Elevation Level

As the slope angle increases, the peak stress values show a decreasing trend. The impact of slope angle changes on stress distribution diminishes with increasing elevation, as illustrated in Figures 15(a) and 15(b). As depicted in Figure 15(c), the stress distribution near the shoulder of the slope crest is significantly affected by changes in slope angle, while the rest of the slope crest positions remain almost unchanged.

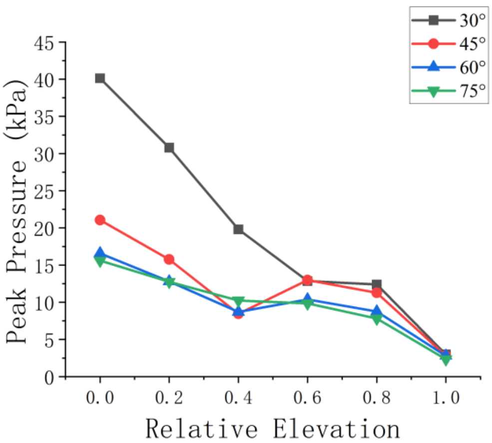

(a) Monitoring point 1_1:1_6

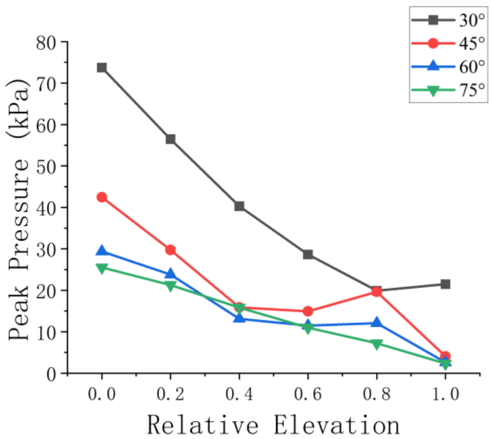

(b) Monitoring point 2_1:2_6

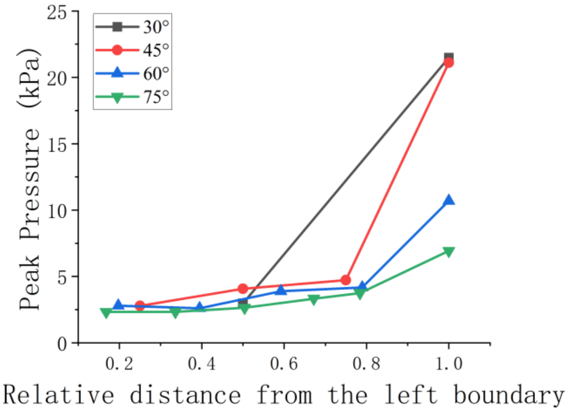

(c) Stress distribution on top of slope

Figure 15. Elevation and Horizontal Variation of Peak Pressure

At the slope surface, peak stress escalates towards the toe, intensifying with slope angle. This suggests that steeper angles focus stress at the slope's base. A significant stress disparity exists across slopes of different angles, with a 75° slope experiencing peak stress at the toe 6.6 times higher than a 30° slope. Steeper slopes, like those at 75°, show considerably higher stresses at the base, with toe stress being 96 times higher than at the shoulder. The influence of slope angle on stress diminishes beyond 40 meters from the base, where stress curves for various angles begin to align, indicating a reduced effect of slope angle at these distances. Peak stress at the toe increases with slope angle, and here, stress distribution is not determined by seismic wave intensity. Given the high peak stress at the base and its independence from seismic intensity, implementing stability measures in this region is crucial for landslide risk reduction. Thus, in slope design, employing reinforcement solutions like retaining walls or support structures is essential.

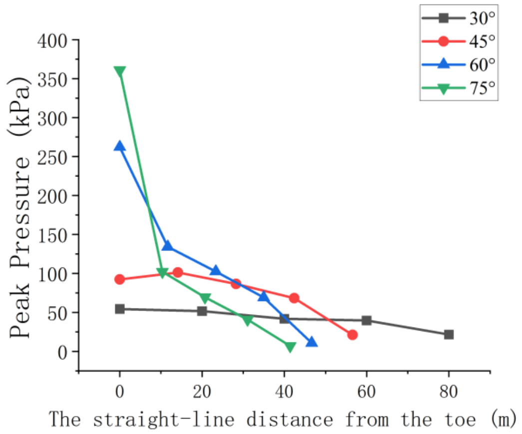

Figure 16. Variability in Peak Displacement Distribution Relative to the Distance from the Slope Toe

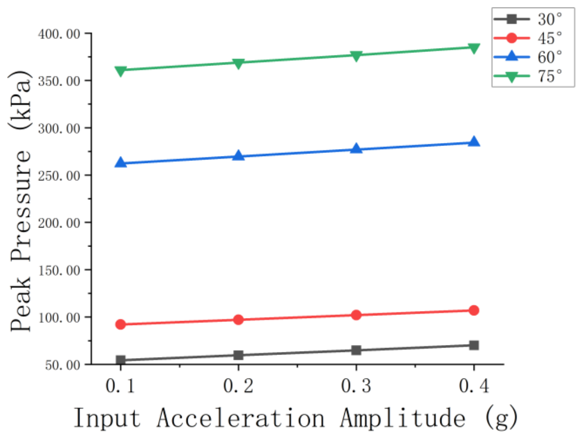

Figure 17. Variability in Peak Displacement Distribution Relative to the Input Acceleration Amplitude

5. Conclusions

(1) The Peak Ground Acceleration (PGA) on slopes shows an overall increasing trend with elevation, reaching its maximum at the slope crest, indicating a progressive increase in acceleration amplification from the base to the top of the slope. Additionally, at the same elevation, PGA decreases as the slope angle increases, with the PGA at slope surface monitoring points being higher than that at internal points, demonstrating a clear trend towards surficial effects.

(2) The PGA at the slope surface shows a trend of first decreasing and then increasing with distance from the slope toe, with this pattern shifting significantly in spatial distribution as the slope angle increases.

(3) The peak displacement shows a trend of first decreasing and then increasing with relative elevation on the slope, particularly sensitive in the relative elevation range of 0.6 to 0.8, where displacement response becomes more sensitive to increases in seismic acceleration. Moreover, the peak displacement increases near the slope surface, reflecting the higher freedom of movement for materials near the slope surface. The effect of slope angle on displacement is significant, particularly when the angle reaches or exceeds 60°, at which point the displacement mechanism appears to change, and peak displacement decreases as the slope angle increases.

(4) The steepness of the slope affects the amplification or attenuation of seismic waves passing through the slope structure, with steeper slopes potentially causing wave focusing phenomena that lead to significant increases in displacement at distant ends, whereas gentler slopes exhibit greater stability under dynamic actions.

(5) The peak stress values decrease with increasing elevation, and this change becomes more pronounced with increasing load intensity. This suggests that the top of the slope, being closer to the

free surface and less constrained, experiences greater seismic load effects, allowing materials to release energy through larger deformations, resulting in relatively lower peak stress values.

(6) An increase in slope angle shifts the stress concentration area from the mid-slope towards the toe, significantly affecting stress distribution at the slope foot, especially at greater angles where the peak stress at the slope foot significantly increases, while the effect of slope angle decreases with distance from the slope foot. Therefore, in the design of slopes, especially steep ones, stability measures at the slope foot, such as retaining walls or support structures, are crucial to reduce landslide risk.

This study systematically examined how slope angle and height affect slope PGA, displacement, and stress distribution under seismic activity, revealing the complex and predictable nature of slope responses. It highlighted the significant effects of slope angle on these factors, guiding slope design and seismic stability. Future research should validate and deepen understanding of these mechanisms through physical and numerical experiments, integrating both to gain comprehensive insights. It should also assess the impact of various soil conditions and complex seismic inputs to improve model accuracy and practicality, thereby enhancing guidance for slope design and earthquake preparedness.

References

[1] Pal, S., P.R. Hanmaiahgari and B.W. Karney, An Overview of the Numerical Approaches to Water Hammer Modelling: The Ongoing Quest for Practical and Accurate Numerical Approaches. WATER, 2021. 13(11).

[2] Yin, D., et al., Numerical analysis of the seismic hazard in Sichuan-Yunnan region. CHINESE JOURNAL OF GEOPHYSICS-CHINESE EDITION, 2022. 65(5): p. 1612-1627.

[3] Fan, X., et al., Coseismic landslides triggered by the 8th August 2017 M s 7.0 Jiuzhaigou earthquake (Sichuan, China): factors controlling their spatial distribution and implications for the seismogenic blind fault identification. Landslides, 2018. 15: p. 967-983.

[4] Chen, Z., et al., The September 16, 2017, Linjiabang landslide in Wanyuan County, China: preliminary investigation and emergency mitigation. Landslides, 2020. 17(1): p. 191-204.

[5] Bolla, A. and P. Paronuzzi. Seismic analysis of a limestone rock slope through numerical modelling: Pseudo-static vs. non-linear dynamic approach. 2021: IOP Publishing.

[6] Guo, M., X. Ge and S. Wang, Slope stability analysis under seismic load by vector sum analysis method. Journal of Rock Mechanics and Geotechnical Engineering, 2011. 3(3): p. 282-288.

[7] Qin, C. and S.C. Chian, New perspective on seismic slope stability analysis. International Journal of Geomechanics, 2018. 18(7): p. 06018013.

[8] Fan, F., et al., Three Dimensional Seismic Stability of Earth Slopes Reinforced with Piles. Journal of Disaster Prevention and Mitigation Engineering, (2): p. 394-402.

[9] Wang, Y., et al., Insights into the kinematics and dynamics of the Luanshibao rock avalanche (Tibetan Plateau, China) based on its complex surface landforms. Geomorphology, 2018. 317: p. 170-183.

[10] Khan, S., et al., The impact of topography on seismic amplification during the 2005 Kashmir earthquake. Nat. Hazards Earth Syst. Sci., 2020. 20(2): p. 399-411.

[11] LIANG, J., et al., Initiation mechanism of earthquake-induced large landslides considering structural damage. Chinese Journal of Geotechnical Engineering, 2021. 43(6): p. 1039-1049.

[12] Xu, W., L. Wang and K. Cheng, The Failure and River Blocking Mechanism of Large-Scale Anti-dip Rock Landslide Induced by Earthquake. Rock Mechanics and Rock Engineering, 2022. 55(8): p. 4941-4961.

[13] Qi, S., J. He and Z. Zhan, A single surface slope effects on seismic response based on shaking table test and numerical simulation. Engineering Geology, 2022. 306: p. 106762.